Biocompatible Label-Free Detection of Carbon Black Particles by
Femtosecond Pulsed Laser Microscopy

Peer-reviewed author version

BOVE, Hannelore; Steuwe, Christian; Fron, Eduard; SLENDERS, Eli; D'HAEN, Jan;
Fujita, Yasuhiko; Uji-i, Hiroshi; VAN DE VEN, Martin; Roeffaers, Maarten &
AMELOOT, Marcel (2016) Biocompatible Label-Free Detection of Carbon Black
Particles by Femtosecond Pulsed Laser Microscopy. In: NANO LETTERS, 16 (5), p. 3173-3178.

# Biocompatible Label-free Detection of Carbon Black Particles by Femtosecond Pulsed Laser Microscopy

*Hannelore Bové[‡1,2], Christian Steuwe[‡2], Eduard Fron[3], Eli Slenders[1], Jan D'Haen[4], Yasuhiko Fujita[3], Hiroshi Uji-i[3,5], Martin vandeVen[1], Maarten Roeffaers[2*], and Marcel Ameloot[1*]*

[1] Biomedical Research Institute, Hasselt University, Agoralaan Building C, 3590 Diepenbeek, Belgium

[2] Centre for Surface Chemistry and Catalysis, KU Leuven, Celestijnenlaan 200F, 3001 Leuven, Belgium

[3] Department of Chemistry, KU Leuven, Celestijnenlaan 200F, 3001 Leuven, Belgium

[4] Institute for Material Research, Hasselt University, Wetenschapspark 1, 3950 Diepenbeek, Belgium

[5] Research Institute for Electronic Science, Hokkaido University, N20W10, Kita-Ward Sapporo 001-0020, Japan

[‡] These authors contributed equally to this work

[*] maarten.roeffaers@biw.kuleuven.be and marcel.ameloot@uhasselt.be

22    ABSTRACT While adverse health effects of carbon black (CB) exposure are generally

23    accepted, a direct, label-free approach for detecting CB particles in fluids and at the cellular

24    level is still lacking. Here, we report non-incandescence related white-light (WL) generation

25    by dry and suspended carbon black particles under illumination with femtosecond (fs) pulsed

26    near-infrared light as a powerful tool for the detection of these carbonaceous materials. This

27    observation is done for four different CB species with diameters ranging from 13 to 500 nm,

28    suggesting this WL emission under fs near-infrared illumination is a general property of CB

29    particles. As the emitted radiation spreads over the whole visible spectrum, detection is

30    straightforward and flexible. The unique property of the described WL emission allows

31    optical detection and unequivocal localization of CB particles in fluids and in cellular

32    environments while simultaneously co-localizing different cellular components using various

33    specific fluorophores as shown here using human lung fibroblasts. The experiments are

34    performed on a typical multiphoton laser-scanning microscopy platform, widely available in

35    research laboratories.

36

37    TEXT Carbon black (CB) consists of aciniform aggregates of primary particles with an

38    elemental carbon content greater than 97 %.[1, 2] It is produced through well controlled

39    incomplete combustion of organics like heavy petroleum or vegetable oil. This distinguishes

40    CB from soot or black carbon, the unwanted by-product released during incomplete

41    combustion processes such as in the exhausts of diesel engines and one of the main

42    contributing factors to atmospheric particulate pollution.[2, 3] Nonetheless, due to the

43    (physico)chemical similarity CB is widely used as a model compound for soot.[4, 5] The total

44    global black carbon emission was estimated to be approximately 8.5 million tons after having

45    constantly increased throughout the preceding decade.[6-8] As a consequence of the increasing

3

46    environmental and occupational exposure to these carbonaceous particles, deeper insight into

47    the (eco-) toxicological impact of these materials is of critical importance.

48

49    So far however, no experimental methods have been reported that enable direct detection of

50    carbon black/black carbon in relevant samples such as polluted water and consumer products

51    as well as exposed cells and body fluids. To date, only measurements[9-11] in polluted air (see

52    reference 9 for an overview) such as absorption photometry and laser induced incandescence

53    (LII) have been used to determine particle concentrations or alternatively labeling methods[12-

54    14] have been explored such as the technetium-99-m radionuclide labeling in epidemiological

55    studies and toxicology research.

56

57    In LII, the emission from carbonaceous materials has been linked to black-body radiation

58    from the severely heated CB particles,[15] *i.e.* incandescence. Already various models have

59    been proposed to explain the origin of incandescence and its dependence on illumination

60    power and pulse duration.[16-18] Recently, substantial scientific efforts have focused on white

61    light (WL) emission from carbonaceous materials including graphene[19], fullerenes[20] and

62    carbon nanotubes[21]. Also for these materials the emitted radiation has been linked to

63    incandescence. However, visible emission from CB particles in solution and biological matter

64    has so far not been sufficiently explored, despite reports of CB suspensions serving as optical

65    limiters and nonlinear scatterers due to their broadband and flat absorption.[16, 17] The

66    interpretation of these effects is not straightforward as they strongly depend on the

67    experimental conditions.[22] Recently, luminescence of carbon particles has been described but

68    this phenomenon seems to be limited to carbon nano-dots, *i.e.* carbon nanoparticles with sizes

69    below 10 nm.[23, 24]

70

71 To the best of our knowledge, we report here for the first time non-incandescence related WL

72 emission of CB particles in aqueous environments under femtosecond pulsed illumination

73 using a multiphoton laser-scanning microscope and demonstrate its potential in a biological

74 context. This label-free approach to directly visualize CB offers additional advantages

75 (schematic representation in Figure 1A) such as inherent 3D sectioning and high imaging

76 depths owing to the multiphoton approach. We anticipate that this method will play an

77 important role in health related studies where the impact and role of CB particles is to be

78 assessed at the organism, tissue, cellular and subcellular level.

79

80 In this study a variety of carbonaceous particles, representative for those to which humans are

81 typically exposed, is used ranging from powders used in copy machines to materials that are

82 typically employed as model for soot. Information on the physico-chemical characteristics of

83 these different commercial CB materials (ufPL, ufP90, CCB and fCB) can be found in Table

84 S1 in the supplementary information (SI). According to manufacturer's data, the aerodynamic

85 diameter of the particles varies between 13 and 500 nm. Transmission electron microscopy

86 (TEM) images (Figure 1B and S1) show the typical appearance of CB consisting of aciniform

87 aggregates of primary carbon particles with arbitrary shape. These TEM images and the

88 results from dynamic light scattering summarized in Table S1 show that CB particles

89 aggregate when suspended in aqueous solutions, and absorb corona proteins from the

90 complete medium onto their surface resulting in an increased hydrodynamic diameter and a

91 zeta-potential corresponding to approximately -20 mV regardless of their native potential. In

92 conclusion, the physico-chemical characteristics of the different CB particles in suspension

93 are similar although when selecting the particles we aimed for as much difference as possible.

94

95
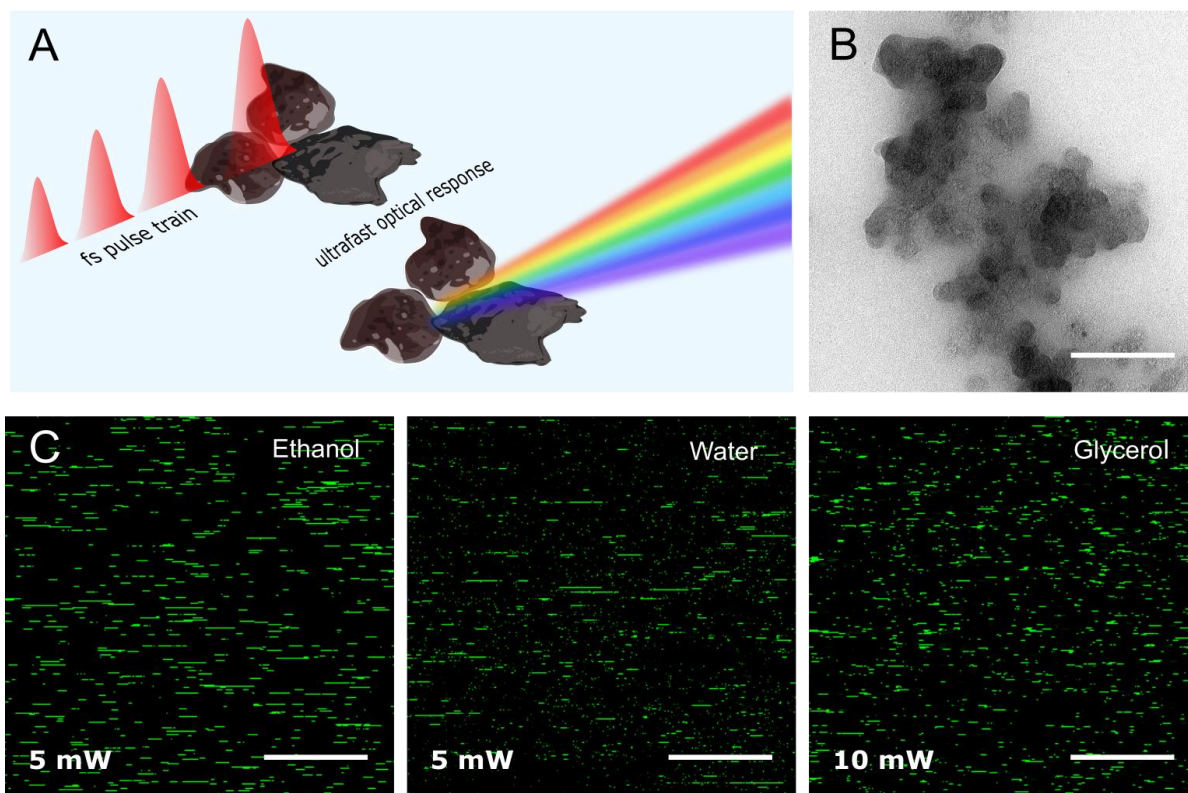
**Figure 1.** (A) Schematic representation of the illumination and emission process of CB particles for the presented detection method. (B) TEM image of an ufPL aggregate. Scale bar: 300 nm. (C) CCB (600 µg/mL) imaging in ultrapure water, ethanol and glycerol at room temperature upon illumination with 5 or 10 mW average laser power at the sample (excitation 810 nm, 80 MHz). Scale bars: 15 µm. Emission band: 450 – 650 nm.

Figure 1C displays CB suspended in ultrapure water, ethanol and glycerol illuminated with a femtosecond laser at 810 nm (150 fs, 80 MHz) and recorded using a commercial multiphoton laser-scanning microscope (detailed information on sample preparation and microscopy modalities can be found in SI). Intense signals were detected with an emission band pass filter of 450 to 650 nm in front of the detector. Depending on the suspension medium, the laser power needs to be adjusted to generate similar emission intensity: in glycerol and immersion oil the illumination power was about twice that of the experiment in ethanol or water (SI, Figure S2). Note the horizontal smearing of the CB particles in Figure 1C (pixel

6

111      dwell time of 1.60 µs, pixel size of 220 nm). This phenomenon is observed at all

112      combinations of scan speeds and zooms (data not shown), suggesting susceptibility of the

113      particles to optical trapping under these conditions. This hypothesis is further supported by

114      the absence of this smearing when CB particles are embedded in polydimethylsiloxane

115      (Figure S3). Trapping by femtosecond laser pulses has already been shown for other types of

116      nanoparticles.[25, 26]

117

118      Additional spectroscopic measurements were performed to investigate the observed visible

119      light emission under femtosecond near-infrared illumination.

120

121      Firstly, we rule out photoluminescence (PL) reported for very small carbonaceous particles

122      (below 10 nanometer)[23, 24, 27] as a cause of the observed emission. Carbonaceous particles, in

123      particular soot, consist of aggregated particles that are heterogeneous in nature[28] and

124      therefore contain multiple absorbing species possibly responsible for radiative transitions.

125      The extinction spectra of aqueous suspensions of the CB particles considered here cover the

126      whole visible range (Figure 2A), presumably due to a continuum of electronic states in the

127      amorphous carbon. The slight increase of the extinction towards lower wavelengths for the

128      two smaller particles (ufPL and ufP90) is likely due to increased light scattering.

129
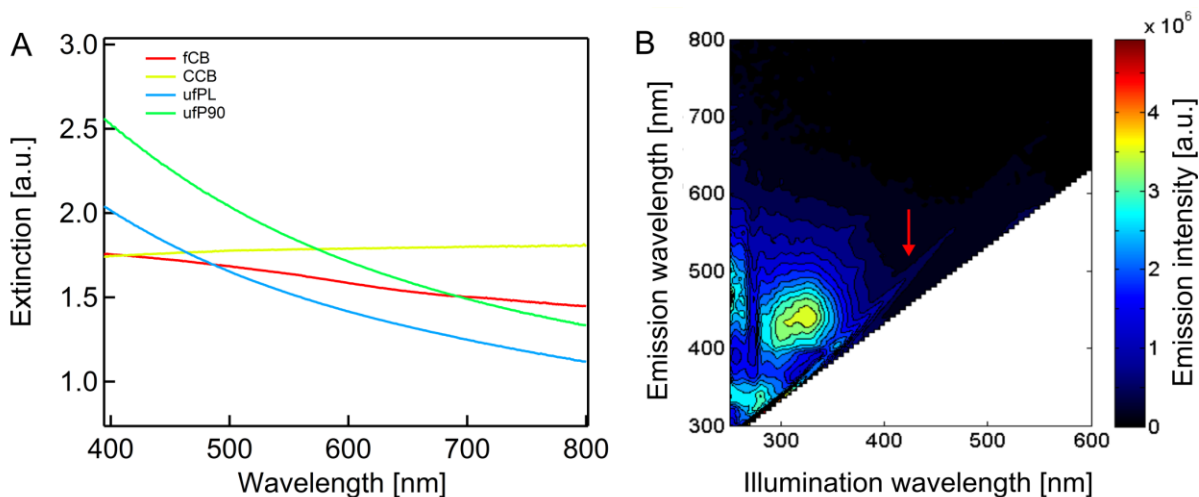
130

131 **Figure 2.** (A) Extinction spectra of aqueous CB suspensions. (B) Two-dimensional

132 excitation-emission plot of ufPL particles in water under single photon excitation with a false

133 color map based on the emission intensity in arbitrary units. The red arrow points towards the

134 Raman line of water.

135

136 Two-dimensional single photon excitation-emission plots (Figure 2B) of ufPL (similar plot

137 for fCB: SI, Figure S4) however, show only weak emission; note in comparison the weak

138 Raman line (red arrow) of water, the suspension medium. The luminescence under excitation

139 in the ultraviolet (UV) region (280 – 380 nm) looks similar to the observations described by

140 Kwon *et al.* for carbon nano-dots[29, 30] and hints towards micro-crystalline graphite exhibiting

141 only a low number of tetrahedral $sp^3$-sites[30-32] which is also confirmed by Raman spectra (SI,

142 Figure S5 and Table S2).

143

144
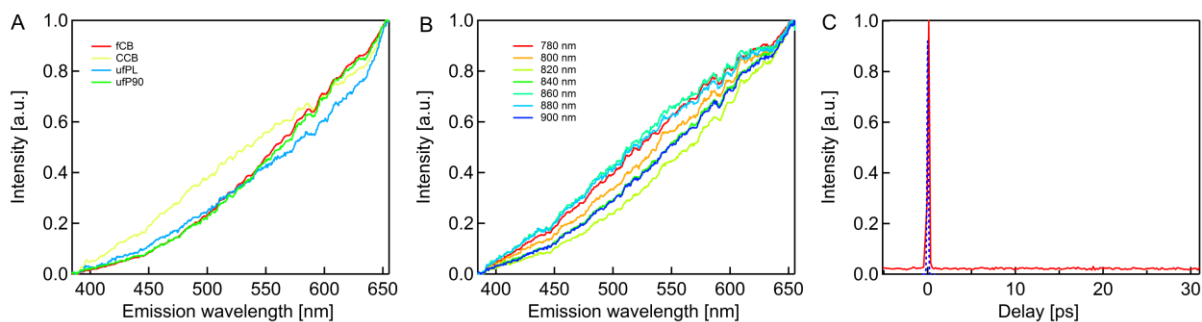
**Figure 3.** (A) Normalized WL emission spectra of aqueous CB particle suspensions using femtosecond 810 nm laser illumination (8 mW, 150 fs, 80 MHz). (B) Normalized WL emission spectra of aqueous ufP90 suspensions recorded at different femtosecond illumination wavelengths. (C) Temporal response of aqueous carbon suspension measured by femtosecond photoluminescence up-conversion experiments. Also shown is the instrument response function (dashed line).

In contrast to single photon excitation, illumination with femtosecond pulsed near-infrared light (810 nm, 150 fs, 80 MHz) generates a strong, feature-less white light emission stretching the whole visible spectrum (Figure 3A and B). This observation was made for all four types of aqueous CB suspensions used in this study and even for dry particles (SI, Figure S6). This WL emission is independent of the illumination wavelength within the range of 780 to 900 nm for a constant average power of 8 mW at the sample (Figure 3B, see also SI, Figure S7).

While PL as visible in Figure 2B cannot explain the strong WL emission observed under femtosecond illumination (Figure 1C, 3A and B), time-resolved investigations are indicative. Using time correlated single photon equipment, an instantaneous nature of the WL radiation is noticed when looking at the picosecond timescale (SI, Figure S8). Also in femtosecond up-conversion experiments with a higher temporal resolution the emitted signal of the CB

9

166    particles is witnessed to be instantaneous (Figure 3C). On further note, illumination with 7 ps

167    pulses results in a strongly reduced luminescence intensity (SI, Figure S9). The WL emission

168    from the suspended CB particles is therefore only efficiently triggered by femtosecond

169    illumination with high peak electromagnetic fields and once the femtosecond illumination

170    pulse ceases, the WL emission terminates immediately.

171

172    The instantaneous nature of the observed signal confirms that we are not dealing with

173    incandescence despite using laser illumination with fluences of about 0.05 J/cm² at 0.1 nJ

174    pulse energy, similar to previous experiments. In those reports, the observed incandescence

175    showed clear decay times in the microsecond time scale regime[31] due to the cooling down of

176    the lattice at these time scales. In fact, heating of the particle lattice, which is required for

177    incandescence, only occurs on a picosecond time scale when remaining non-emitted energy

178    will be converted into lattice vibrations.[32-34] The femtosecond illumination employed here is

179    too fast.

180

181    The observed instantaneous WL emission is also not related to local refractive index changes

182    in the CB nanoparticle environment upon pulse arrival. Gold nanoparticles are for example

183    known to form nanometer-sized bubbles when illuminated with pulsed lasers at laser

184    fluencies similar to those applied here.[31, 35] and those have been observed leading to broad

185    featureless WL emission.[35-38] If a related principle would be underlying the observed WL

186    emission in CB suspension, the emission spectra would be strongly influenced by the

187    surrounding refractive index. However, even dry particles show the same spectral profile as

188    those suspended in water (SI, Figure S6).

189

190      We believe that the observed visible light emission under femtosecond near-infrared

191      illumination is related to the broad anti-Stokes emission with non-linear power dependence

192      that was previously observed by other groups for noble metal nanoparticles. In those

193      experiments, the emission arose from femtosecond illumination of gold and silver particles or

194      nanostructures.[39-42] We can confirm that also the WL emission of CB displays a nonlinear,

195      second order response with respect to the incident power (SI, Figure S10). The WL emission

196      of gold was recently succinctly investigated by Haug *et al.*[43] Here, plasmonic confinement of

197      electric fields in metal along with the small dimensions of the emitting particle can

198      presumably relax symmetry selection and momentum conservation rules to allow for

199      (continuous) intraband dipole transitions, which would otherwise be impossible. The

200      observed emission is independent of the type of metal and the preparation conditions. Even

201      though carbon particles are not metallic in nature and do not show plasmonic modes in the

202      visible or near UV spectral range (see Figure 2A), an electron gas could emerge on arrival of

203      a femtosecond pulse. At very high energies, even plasmons or plasmon-like effects have been

204      discovered with electron energy loss spectroscopy in carbon nanotubes and its parent material

205      graphene[44-46] or in graphitic spheres[47]. Buckminsterfullerene[48] and other carbonaceous

206      materials[49] show strong multiphoton ionization. The intense and spectrally broad absorption

207      of the particles could give rise to this phenomenon, promoting resonant multiphoton

208      transitions leading to ionizations.[50] Therefore, consecutive intraband transitions similar to

209      those noticed in plasmonically active metals could be a valid explanation for the observed

210      results.

211

212      As a result of visible WL generation by carbon black particles under femtosecond pulsed

213      near-infrared illumination, the signal of the particles can easily be combined with various

214      conventional contrast-enhancing fluorophores used to visualize biological features. As shown

215 in Figure 4, the emitted WL can be probed at different wavelengths at laser powers

216 compatible with life cell imaging. Hence, CB detection can be combined with the imaging of

217 cellular compartments stained by different color-label fluorophores (labeling strategy can be

218 found in SI). This simultaneous detection enables unequivocally localization of the particles

219 inside the cells and puts the CB location directly into its biological context.

220
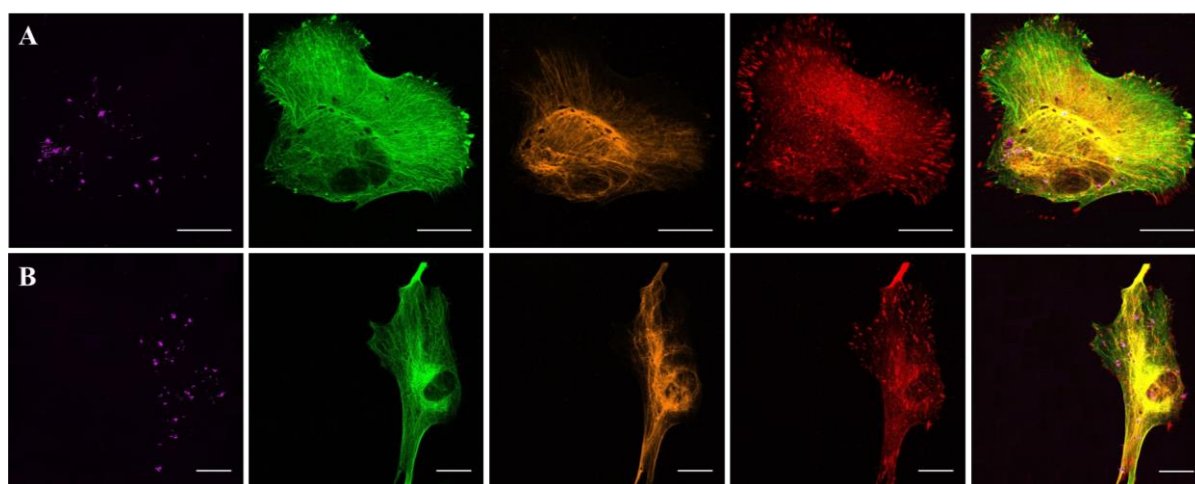


221

222 **Figure 4.** Imaging of cellular compartments of fixed MRC-5 cells stained with commonly

223 utilized fluorophores and in combination with the detection of CCB particles (4 h incubation

224 of 5 µg/cm$^2$ CCB at 37 °C prior to imaging). Emission of the carbonaceous particles can be

225 probed at different wavelengths, here shown at (A) 400 – 410 nm in the non-descanned mode

226 and (B) 650 – 710 nm in descanned mode (4 mW average laser power at the stage). From left

227 to right: CCB particles, tubulin cytoskeleton (Ex/Em 495/519 nm, ~ 3 µW radiant power at

228 the sample), vimentin which is an intermediate filament protein of the cytoskeleton (Ex/Em

229 555/565 nm, ~ 3 µW radiant power at the sample), paxillin expressed at focal adhesions

230 (Ex/Em 650/665 nm, ~ 3 µW radiant power at the sample), and overlay image. Scale bars:

231 25 µm.

232

233    To further illustrate the versatility of the technique in a biological setting, a co-localization

234    study of the tubulin cytoskeleton of MRC-5 lung fibroblasts and engulfed carbon particles

235    was performed (Figure 5). The images show a clear impact of CCB on the architecture of the

236    tubulin cytoskeleton of the cells for an incubation that exceeds four hours at 37 $^{\circ}$C. More

237    specifically, the supporting cytoskeleton network evolves from the commonly observed fiber-

238    like structure to a partial diffuse and holey configuration. The cytoskeletal alteration is also

239    reflected in the overall morphology of the cells. Their appearance changed from the normal

240    bipolar and stretched morphology to a smaller and more irregular shaped one, which is an

241    indication of apoptosis (these biological findings are also true for the other smaller CB

242    particles, for an additional example with ufP90, see SI, Figure S11).[51-53] These images do not

243    only pinpoint the versatility in biological settings but also immediately indicate the social

244    relevance and significance of this detection technique. Potential advantageous information

245    arising from this simultaneous detection comprise the correlations that can be made between

246    the location of the particles and the altered cellular structure (*e.g.,* cytoskeleton and focal

247    adhesions). This makes the observed WL emission an extremely interesting label-free

248    detection mechanism for biomedical research including toxicology and epidemiology.

249
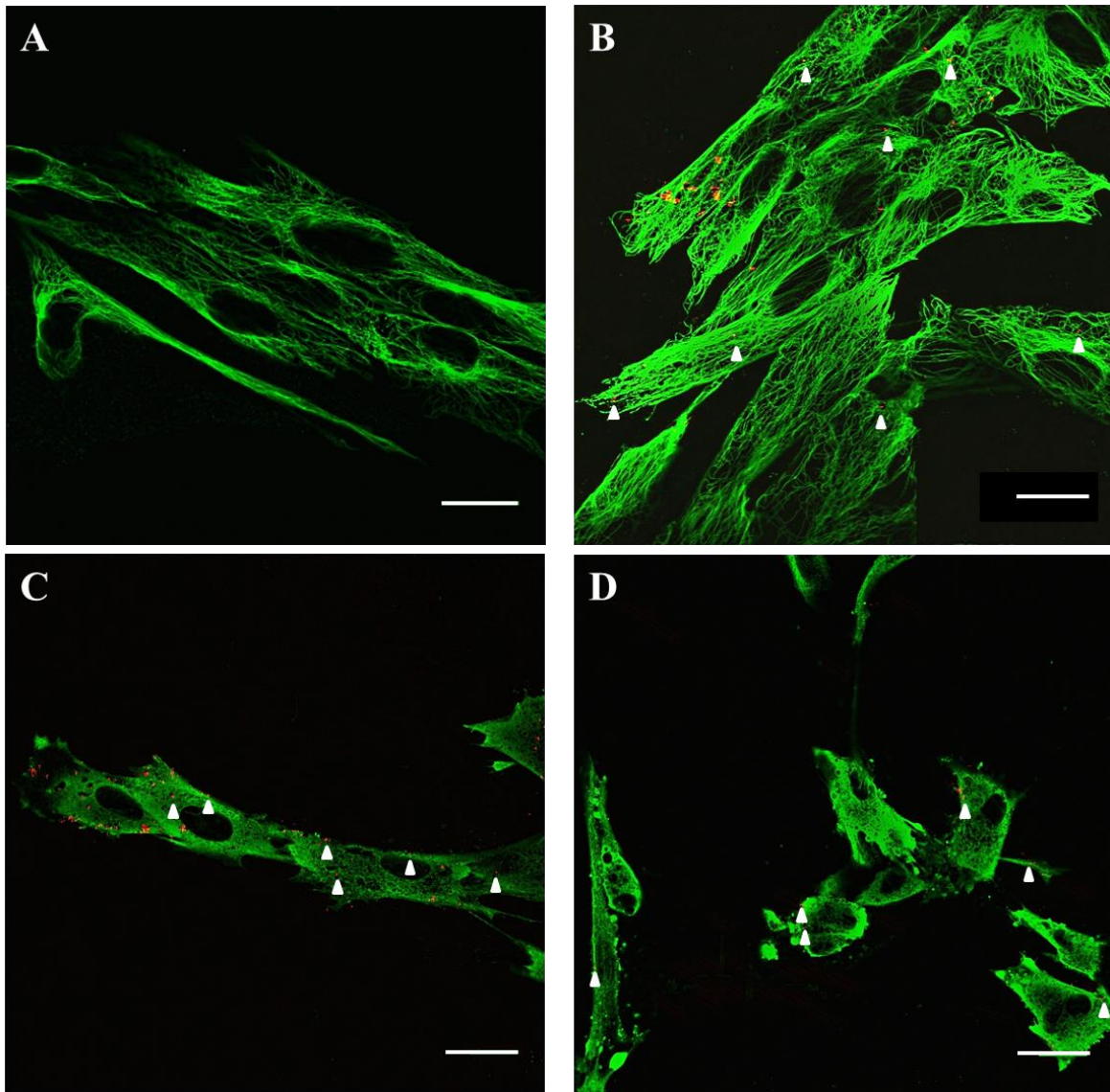
**Figure 5.** Tubulin cytoskeleton (green, Ex/Em 495/519 nm, ~ 3 µW radiant power at the sample) of normal human lung fibroblasts incubated with 5 µg/cm$^2$ CCB particles (red, 4 mW average laser power at the sample, emission detection: 400 – 410 nm in non-descanned mode) at 37 °C. (A) Control cells. (B) 4 h incubation. (C) 8 h incubation. (D) 24 h incubation. Scale bars: 30 µm. Arrow heads: some locations of very small, engulfed CCB particles.

To conclude, femtosecond pulsed illumination of CB followed by detection of emitted WL is a straightforward approach without the need of particular sample pretreatment and which can easily be implemented in multiphoton imaging experiments. The nature of the signal makes it very versatile in terms of choice of additional fluorophores. The ease of the reported

260    approach broadens the potential applicability in the fast growing field of nanotechnology.

261    Additionally, it will advance epidemiological and toxicological studies since this is the first

262    time a technique is described to directly detect carbon black in a biological setting without

263    any additional treatment or labeling required. We anticipate that this technology will make it

264    possible to screen human tissues and body fluids for the presence of CB owing to the

265    multiphoton approach which results in inherent 3D sectioning and high imaging depths. This

266    may eventually lead to valuable information about, for example, the actual uptake and

267    clearance of CB particles by the human body.

ASSOCIATED CONTENT

**Supporting Information**

Detailed methods and supplemental figures. This material is available free of charge via the Internet at http://pubs.acs.org.

AUTHOR INFORMATION

**Corresponding Author**

* (M.R.) E-mail: maarten.roeffaers@biw.kuleuven.be. Phone: +3216-327-449.

* (M.A.) E-mail: marcel.ameloot@uhasselt.be. Phone: +3211-269-233.

**Author Contributions**

‡These authors contributed equally in the performance of the experiments. H.B., C.S., M.R. and M.A. jointly designed and analyzed the experiments. H.B. and C.S. performed most of the experiments. E.F. performed the femtosecond fluorescence up-conversion experiments. E.S. assisted with the time correlated single photon counting. J.D. made the transmission electron microscopy images. H.U. and Y.F. gave their technical support during spectral data collection. M.V. gave theoretical support. The manuscript was written through contributions of all authors. All authors have given approval to the final version of the manuscript.

**Notes**

The authors declare no competing financial interests. Patent application about the described findings was filed on 12/01/2016 in the UK [patent application number 1600564.7].

298

299     REFERENCES

300     1.      ASTM, *American Society for Testing Materials D3053-13a, Standard on*
301             *Terminology Relating to Carbon Black*. ASTM International: West Conshohocken,
302             PA, 2013.

303     2.      Watson, A. Y.; Valberg, P. A. *AIHAJ* **2001,** 62, (2), 218-228.

304     3.      Castro, L.; Pio, C.; Harrison, R. M.; Smith, D. *Atmos. Environ.* **1999,** 33, (17), 2771-
305             2781.

306     4.      Arnal, C.; Alzueta, M.; Millera, A.; Bilbao, R. *Combust. Sci. Technol.* **2012,** 184, (7-
307             8), 1191-1206.

308     5.      Tankersley, C. G.; Bierman, A.; Rabold, R. *Inhal. Toxicol.* **2007,** 19, (8), 621-9.

309     6.      Bond, T. C.; Bhardwaj, E.; Dong, R.; Jogani, R.; Jung, S.; Roden, C.; Streets, D. G.;
310             Trautmann, N. M. *Glob. Biogeochem. Cycles* **2007,** 21, (2).

311     7.      Lamarque, J.-F.; Bond, T. C.; Eyring, V.; Granier, C.; Heil, A.; Klimont, Z.; Lee, D.;
312             Liousse, C.; Mieville, A.; Owen, B. *Atmos. Chem. Phys.* **2010,** 10, (15), 7017-7039.

313     8.      Wang, R., *Global Emission Inventory and Atmospheric Transport of Black Carbon:*
314             *Evaluation of the Associated Exposure*. Springer Theses: Beijing, China, 2015.

315     9.      Chow, J. C.; Watson, J. G.; Doraiswamy, P.; Chen, L.-W. A.; Sodeman, D. A.;
316             Lowenthal, D. H.; Park, K.; Arnott, W. P.; Motallebi, N. *Atmos. Res.* **2009,** 93, (4),
317             874-887.

318     10.     OECD. *Methods of Measuring Air Pollution: Report of the Working Party on*
319             *Methods of Measuring Air Pollution and Survey Techniques*; Organization for
320             Economic Co-operation and Development: Paris, France, 1964.

321     11.     Schulz, C.; Kock, B. F.; Hofmann, M.; Michelsen, H.; Will, S.; Bougie, B.; Suntz, R.;
322             Smallwood, G. *Appl. Phys. B* **2006,** 83, (3), 333-354.

323   12.   Kong, H.; Zhang, Y.; Li, Y.; Cui, Z.; Xia, K.; Sun, Y.; Zhao, Q.; Zhu, Y. *Int. J. Mol.*

324         *Sci.* **2013,** 14, (11), 22529-22543.

325   13.   Wang, H.-f.; Troxler, T.; Yeh, A.-g.; Dai, H.-l. *J. Phys. Chem. C* **2007,** 111, (25),

326         8708-8715.

327   14.   Nemmar, A.; Hoet, P. M.; Vanquickenborne, B.; Dinsdale, D.; Thomeer, M.;

328         Hoylaerts, M.; Vanbilloen, H.; Mortelmans, L.; Nemery, B. *Circulation* **2002,** 105,

329         (4), 411-414.

330   15.   Ferrari, A.; Meyer, J.; Scardaci, V.; Casiraghi, C.; Lazzeri, M.; Mauri, F.; Piscanec,

331         S.; Jiang, D.; Novoselov, K.; Roth, S. *Phys. Rev. Lett.* **2006,** 97, (18), 187401.

332   16.   Belousova, I.; Mironova, N.; Scobelev, A.; Yur'ev, M. *Opt. Commun.* **2004,** 235, (4),

333         445-452.

334   17.   Zelensky, S. *Semicond. Phys. Quantum Electron. Optoelectron.* **2004,** 7, (2), 190-194.

335   18.   Rulik, J. J.; Mikhailenko, N.; Zelensky, S.; Kolesnik, A. *Semicond. Phys. Quantum*

336         *Electron. Optoelectron.* **2007,** 10, (2), 6-10.

337   19.   Strek, W.; Cichy, B.; Radosinski, L.; Gluchowski, P.; Marciniak, L.; Lukaszewicz,

338         M.; Hreniak, D. *Light Sci. Appl.* **2015,** 4, (1), e237.

339   20.   Hamilton, B.; Rimmer, J.; Anderson, M.; Leigh, D. *Adv. Mater.* **1993,** 5, (7-8), 583-

340         585.

341   21.   Imholt, T.; Dyke, C. A.; Hasslacher, B.; Pérez, J. M.; Price, D.; Roberts, J. A.; Scott,

342         J.; Wadhawan, A.; Ye, Z.; Tour, J. M. *Chem. Mater.* **2003,** 15, (21), 3969-3970.

343   22.   Fougeanet, F.; Fabre, J.-C. In *Nonlinear mechanisms in carbon-black suspension in a*

344         *limiting geometry*, MRS Proceedings, 1997; Cambridge Univ. Press: p 293.

345   23.   Li, H.; Kang, Z.; Liu, Y.; Lee, S.-T. *J. Mater. Chem.* **2012,** 22, (46), 24230-24253.

346   24.   Ghosh, S.; Chizhik, A. M.; Karedla, N.; Dekaliuk, M. O.; Gregor, I.; Schuhmann, H.;

347         Seibt, M.; Bodensiek, K.; Schaap, I. A.; Schulz, O. *Nano Lett.* **2014,** 14, (10), 5656-

348         5661.

349   25.   Usman, A.; Chiang, W. Y.; Masuhara, H. *Sci. Prog.* **2013,** 96, (Pt 1), 1-18.

350   26.   Usman, A.; Chiang, W.-Y.; Masuhara, H. In *Femtosecond trapping efficiency*

351         *enhanced for nano-sized silica spheres*, 2012; pp 845833-845833-7.

352   27.   Li, Q.; Ohulchanskyy, T. Y.; Liu, R.; Koynov, K.; Wu, D.; Best, A.; Kumar, R.;

353         Bonoiu, A.; Prasad, P. N. *J. Phys. Chem. C* **2010,** 114, (28), 12062-12068.

354   28.   Bond, T. C.; Bergstrom, R. W. *Aerosol Sci. Technol.* **2006,** 40, (1), 27-67.

355   29.   Kwon, W.; Do, S.; Kim, J.-H.; Jeong, M. S.; Rhee, S.-W. *Sci. Rep.* **2015,** 5.

356   30.   Carpene, E.; Mancini, E.; Dallera, C.; Schwen, D.; Ronning, C.; De Silvestri, S. *New*

357         *J. Phys.* **2007,** 9, (11), 404.

358   31.   Michelsen, H. A. *The Journal of chemical physics* **2003,** 118, (15), 7012-7045.

359   32.   Link, S.; El-Sayed, M. A. *J. Phys. Chem. B* **1999,** 103, (40), 8410-8426.

360   33.   Ahmadi, T. S.; Logunov, S. L.; El-Sayed, M. A. *J. Phys. Chem.* **1996,** 100, (20),

361         8053-8056.

362   34.   Hodak, J.; Martini, I.; Hartland, G. V. *Chem. Phys. Lett.* **1998,** 284, (1), 135-141.

363   35.   Kotaidis, V.; Dahmen, C.; Von Plessen, G.; Springer, F.; Plech, A. *The Journal of*

364         *chemical physics* **2006,** 124, (18), 184702.

365   36.   Lapotko, D. *Opt. Express* **2009,** 17, (4), 2538-2556.

366   37.   Lapotko, D. *Int. J. Heat Mass Trans.* **2009,** 52, (5), 1540-1543.

367   38.   Lukianova-Hleb, E. Y.; Sassaroli, E.; Jones, A.; Lapotko, D. O. *Langmuir* **2012,** 28,

368         (10), 4858-4866.

369   39.   Kim, H.; Sheps, T.; Taggart, D. K.; Collins, P. G.; Penner, R. M.; Potma, E. O. In

370       *Coherent anti-Stokes generation from single nanostructures*, SPIE BiOS: Biomedical

371       Optics, 2009; International Society for Optics and Photonics: pp 718312-718312-8.

372   40.   Beversluis, M. R.; Bouhelier, A.; Novotny, L. *Phys. Rev. B* **2003,** 68, (11), 115433.

373   41.   Danckwerts, M.; Novotny, L. *Phys. Rev. Lett.* **2007,** 98, (2), 026104.

374   42.   Palomba, S.; Danckwerts, M.; Novotny, L. *J. Opt. A-Pure Appl. Op.* **2009,** 11, (11),

375       114030.

376   43.   Haug, T.; Klemm, P.; Bange, S.; Lupton, J. M. *Phys. Rev. Lett.* **2015,** 115, (6),

377       067403.

378   44.   Kramberger, C.; Hambach, R.; Giorgetti, C.; Rümmeli, M.; Knupfer, M.; Fink, J.;

379       Büchner, B.; Reining, L.; Einarsson, E.; Maruyama, S. *Phys. Rev. Lett.* **2008,** 100,

380       (19), 196803.

381   45.   Ajayan, P.; Iijima, S.; Ichihashi, T. *Phys. Rev. B* **1993,** 47, (11), 6859.

382   46.   Pichler, T.; Knupfer, M.; Golden, M.; Fink, J.; Rinzler, A.; Smalley, R. *Phys. Rev.*

383       *Lett.* **1998,** 80, (21), 4729.

384   47.   Stöckli, T.; Bonard, J.-M.; Châtelain, A.; Wang, Z. L.; Stadelmann, P. *Phys. Rev. B*

385       **1998,** 57, (24), 15599.

386   48.   Ding, D.; Compton, R.; Haufler, R.; Klots, C. *J. Phys. Chem.* **1993,** 97, (11), 2500-

387       2504.

388   49.   Pratt, S. T.; Dehmer, J. L.; Dehmer, P. M. *J. Chem. Phys.* **1985,** 82, (2), 676-680.

389   50.   Streibel, T.; Zimmermann, R. *Annu. Rev. Anal. Chem.* **2014,** 7, 361-381.

390   51.   Hussain, S.; Thomassen, L. C.; Ferecatu, I.; Borot, M.-C.; Andreau, K.; Martens, J.

391       A.; Fleury, J.; Baeza-Squiban, A.; Marano, F.; Boland, S. *Part. Fibre Toxicol.* **2010,**

392       7, (1), 1.

393  52.  Sydlik, U.; Bierhals, K.; Soufi, M.; Abel, J.; Schins, R. P.; Unfried, K. *Am. J. Physiol.*

394  *Lung Cell. Mol. Physiol.* **2006,** 291, (4), L725-L733.

395  53.  Bortner, C.; Cidlowski, J. *Cell Death Differ.* **2002,** 9, (12), 1307-1310.

396